Component method for steel column bases

František Wald

Czech Technical University, Faculty of Civil Engineering, Prague, Czech Republic

Zdeněk Sokol

Czech Technical University, Faculty of Civil Engineering, Prague, Czech Republic

Martin Steenhuis †

Eindhoven University of Technology, Faculty of Architecture, Building and Planning, the Netherlands

Jean-Pierre Jaspart

Université de Liège, Institut du Génie Civiel Départemant MSM, Belgium

This paper presents the application of the component method to steel column bases. The decomposition of the connection into components is described. An analytical model is presented to determine the moment resistance and the rotational stiffness of column bases under axial forces. The analytical model is verified with test results. A sensitivity study of the base plate thickness and the anchor bolt length is presented.

Key words: Base plate, component method, analytical model, tests, design model

1 Introduction

Column bases are one of the least studied structural elements. Compared to beam-to-column connections, where more then a thousand tests are published, the number of tests on column bases is limited to about 200. The level of description of the measured data is varying. In recent years, plastic analysis, see [1] and [2], have replaced the traditional elastic approaches to the column base design. Eurocode 3 (pre-norm ENV) Section 6, contains principles, and Annex L contains detailed application rules for the resistance of column bases subject to the axial loads. In version of a draft of norm, prEN, eccentrically loaded base plates are included [3].

Classical approaches [4], [5], and [6] of the design of the moment-resisting bases involve an elastic analysis, based on the assumption that the section consisting of anchor bolts and a base plate in compression remains plane. By solving equilibrium equations, the maximum stress in the concrete (based on a triangular distribution of stress), the extent of the stress block and the tension in the holding down assemblies may be determined. Whilst this procedure has proved to be satisfactory in service over many years, the approach ignores the flexibility of the base plate in bending, the holding down assemblies and the concrete, see [7] and [8]. The traditional elastic models for column base design give a safe, conservative solution with relatively thick base plates and expensive holding down (anchoring) systems.

Base fixity has an important effect on the calculated frame behaviour, particularly on frame deflections [9]. Traditionally, column bases are modelled as either pinned or as fixed, whilst the reality lies somewhere within these two extremes. The opportunity to either calculate or to model the base stiffness in analysis was not available.

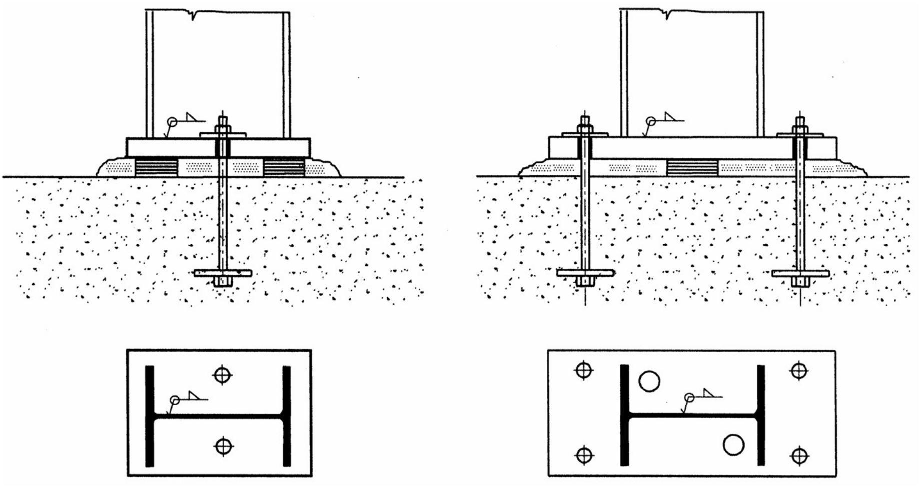

Figure 1: The column base detailing, configured with two and four anchor bolts. The headed anchor bolts and the un-stiffened base plates are shown as one example of a fixing system.

The paper describes the application of the component method to determine the column base behaviour in terms of the moment resistance and the stiffness. The paper is based on the European developments in the column base modelling prepared in the COST Cl project [10]. By this project three basic prediction models [11], [12] and [13] were combined to reach the accepted. The influence of the foundation behaviour is not considered in this paper.

2 Component method

The component method consists of the following issues: identification, characterisation, assembly, classification and modelling. The identification is the process of decomposing a joint in different components. Figure 2 shows the components of a column base. In the characterisation of each component, the relevant mechanical properties are determined: the resistance, the stiffness and the deformation capacity. In the assembly, the mechanical properties of the components are combined in order to determine the resistance, the stiffness and the rotational capacity of the joint. The joints are classified in terms of the resistance, the deformation capacity or the stiffness. The purpose of the classification is the simplification of the joint behaviour under the frame analysis, for instance by classifying for the stiffness as rigid. Modelling is required to determine how the (non-linear) mechanical properties of the joint are taken into account in the frame analysis. This paper focuses on the assembly procedure of column bases and the behaviour of component is expected to be fully described.

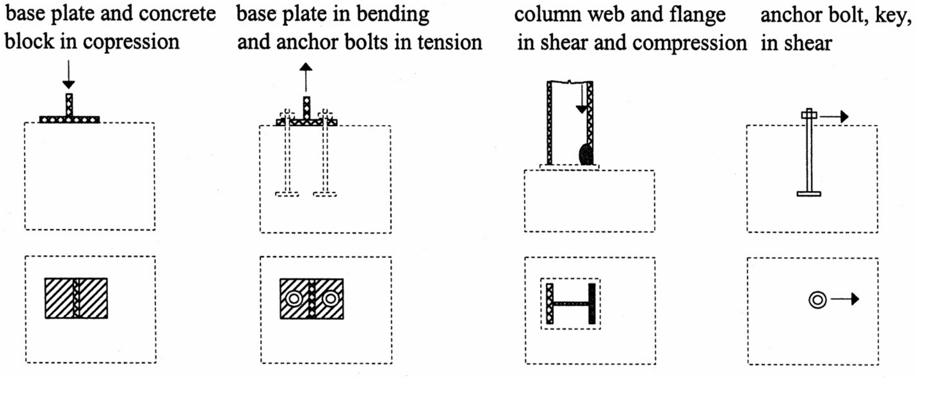

Figure 2: Decomposition of the column base with the base plate into the major components

The component behaviour was studied separately by a series of tests on components, Finite Element (FE) simulations and related sensitivity studies [16]. The component stiffness and resistance are determined for the base plate and concrete block in compression, the base plate in bending and the anchor bolts in tension, and the anchor bolts in shear.

3 Assembling

3.1 Proportional and non-proportional loading

A characteristic of column bases is that they are loaded by a combination of the shear forces, the axial forces and the bending moments. The axial force has an influence on the moment resistance of the joint. Two typical cases are distinguished. In case of the non-proportional loading, the axial force is applied to the base plate connection first, and then the moment is applied. In the case of the proportional loading, the axial force and the bending moment are applied simultaneously to the joints, with a constant ratio between the bending moment and the axial force (this is also called the eccentricity). Figure 6 shows the moment-rotation curve for a typical column base connection with proportional and non-proportional loading. The figure shows that in case of non-proportional loading, the stiffness of the base plate joint is higher compared to the non-proportional loading. This is due to the presence of the axial force in the column, which keeps the base plate in the contact with the concrete in case of low bending moments. Only when the axial force and the moment have the same value, the rotations in the joint are identical for both loading cases.

3.2 Modelling of bending resistance

An equivalent T-stub is used to model the effective area representing the flexible base plate as a rigid one. An effective width c describes the T-stub behaviour see [3]. The acting bending moment and the axial force are shown at Figure 3. A plastic distribution of the internal forces may be calculated based on the resistance of a tension part $F_{t,Rd}$ the position of the neutral axes, the bending resistance M_{Rd} and the axial force N_{Sd} , see Figure 3.

3.3 Simplified modelling of bending resistance and rotational stiffness

The simplified model for the bending resistance and the rotational stiffness takes the effective area under the flanges into account [12] only. The effective area under the column web is neglected, as shown in Figure 4. The compression force is assumed to act at the centre of the flange in compression, also in the cases of the limited outstand of the base, see Figure 4c and 4d. The tensile force is located at the anchor bolts or midway between the bolts when there are two rows of tension bolts, as shown in Figure 4a.

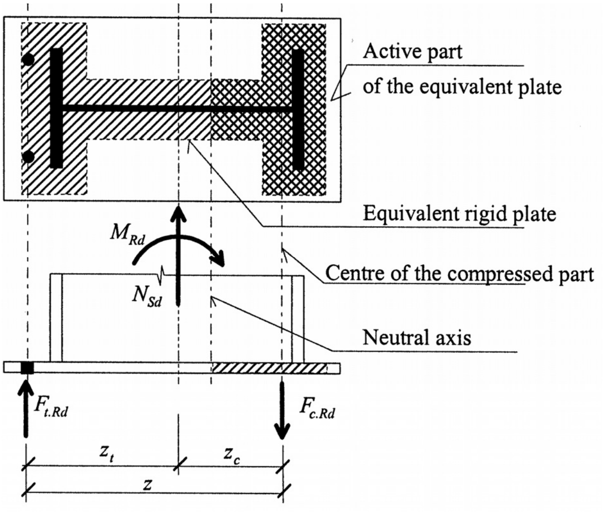

Figure 3: Force equilibrium of the column base

The equilibrium of forces may be calculated based on Figure 4. The base plate with four anchor bolts, see Figure 4a, and with two anchor bolts inside the column, see Figure 4c, are shown as an example of application of method. A special case is the column bases with anchor bolts placed on axes of symmetry of the plate. The base plate with one row of anchor bolts in the outstand of base plate, see Figure 3 and 5a, may be modelled in a similar way. The forces act in bolt lines. The outstand smaller, see Figure 4c and 4d, compare to c is changing the size of the equivalent rigid plate but not the lever arm. The forces represent the resistances of the components in the tension, $F_{t,l,Rd}$ and in the compression, $F_{c,l,Rd}$, $F_{c,r,Rd}$. The component resistances are calculated separately [9]. From Figure 4a and 4c for the eccentricity $e = M_{Sd} / N_{Sd} \leq -z_{c,r}$ the following formula can be derived

$$\frac{M_{sd}}{z} + \frac{N_{Sd}\, z_{c,r}}{z} \leq F_{t,l} \tag{1}$$

and

$$\frac{M_{sd}}{z} - \frac{N_{Sd}\, z_{t,l}}{z} \leq F_{c,r} \,. \tag{2}$$

Since $e = M_{Sd} / N_{Sd} = M_{Rd} / N_{Rd}$, Eq. (1) and (2) can be rewritten as

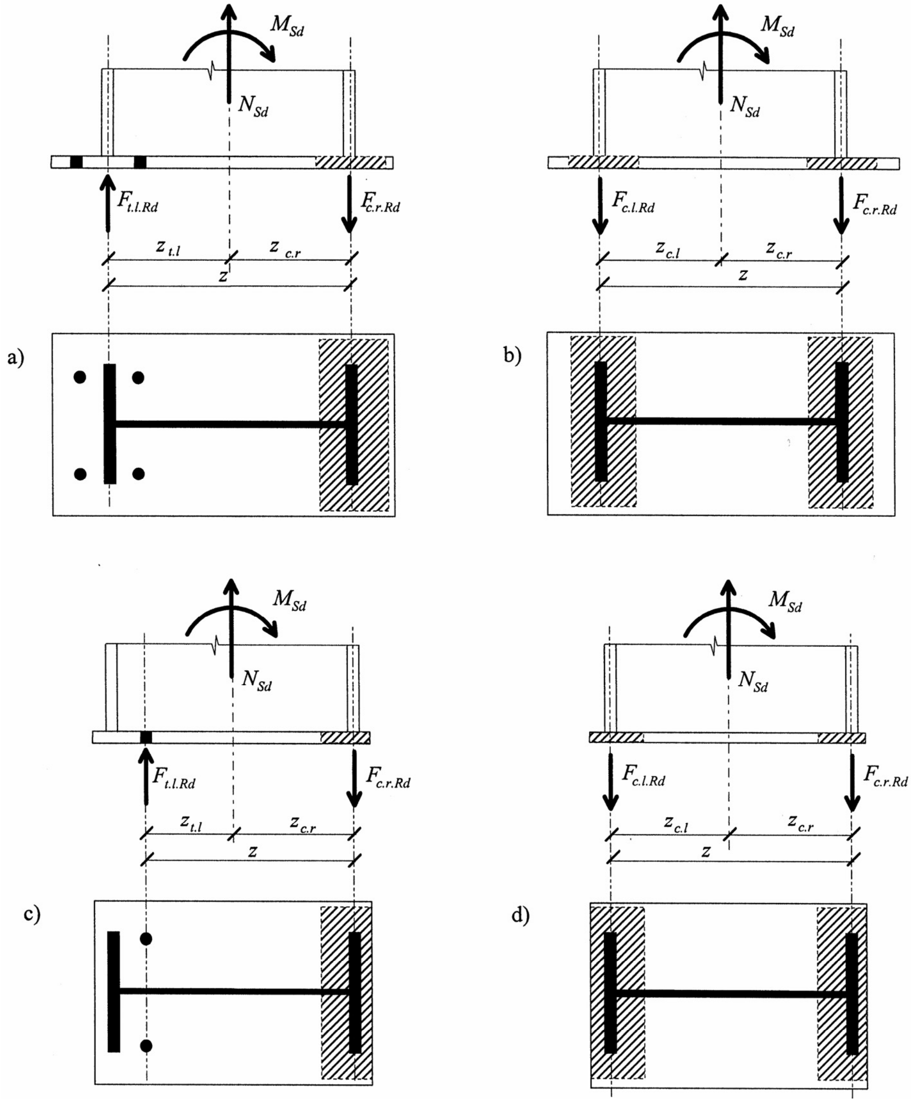

Figure 4: Equilibrium of forces of the base plate, with the effective area under the flanges only;

a) two rows of the anchor bolts in tension;

b) no net tension on the base plate;

c) one row of the anchor bolts in tension, the limited plate outstand;

d) no net tension, the limited plate outstand

$$M_{Rd} = \min \begin{Bmatrix} \dfrac{F_{t,l}\, z}{\dfrac{z_{c,r}}{e} + 1} \\ \dfrac{-F_{c,r}\, z}{\dfrac{z_{t,l}}{e} - 1} \end{Bmatrix} . \tag{3}$$

For the eccentricity $e = M_{Sd} / N_{Sd} > -z_{c,r}$, see Figure 4b and 4d, there is no tension force in the anchor bolt but both parts of the connection are under compression. In this case, the equation may be rewritten as

$$M_{Rd} = \min \begin{Bmatrix} \dfrac{-F_{c,l}\, z}{\dfrac{z_{c,r}}{e} + 1} \\ \dfrac{-F_{c,r}\, z}{\dfrac{z_{c,l}}{e} - 1} \end{Bmatrix} . \tag{4}$$

The bending stiffness of a base plate shell be evaluated based on the deformation stiffness of the main components, see [7] and [10].

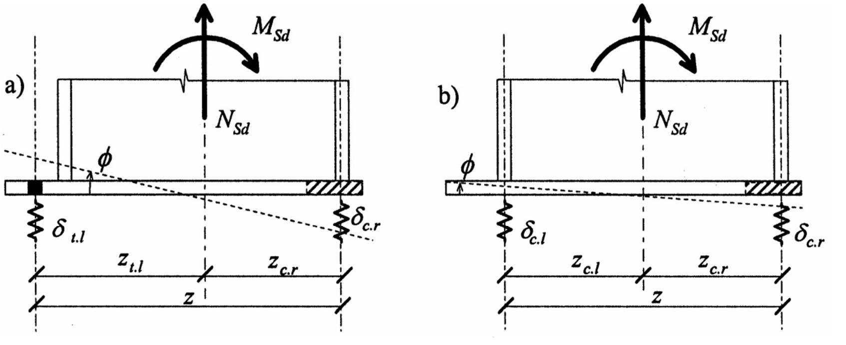

Figure 5: The mechanical model of the base plate

The elastic deformation may be expressed, see Figure 5, as [12]

$$\delta_{t,l} = \frac{\dfrac{M_{Sd}}{z} + \dfrac{N_{Sd}\, z_{c,r}}{z}}{E\, k_{t,l}} = \frac{M_{Sd} + N_{Sd}\, z_{c,r}}{E\, z\, k_{t,l}} \ , \tag{5}$$

$$\delta_{c,r} = \frac{\dfrac{M_{Sd}}{z} - \dfrac{N_{Sd}\, z_{t,l}}{z}}{E\, k_{c,r}} = \frac{M_{Sd} + N_{Sd}\, z_{t,l}}{E\, z\, k_{c,r}} \ , \tag{6}$$

and the column base rotation is

$$\phi = \frac{\delta_{t,l} + \delta_{c,r}}{z} = \frac{1}{E z^2} \left(\frac{M_{Sd} + N_{Sd}\, z_{c,r}}{k_{t,l}} + \frac{M_{Sd} - N_{Sd}\, z_{t,l}}{k_{c,r}} \right) . \tag{7}$$

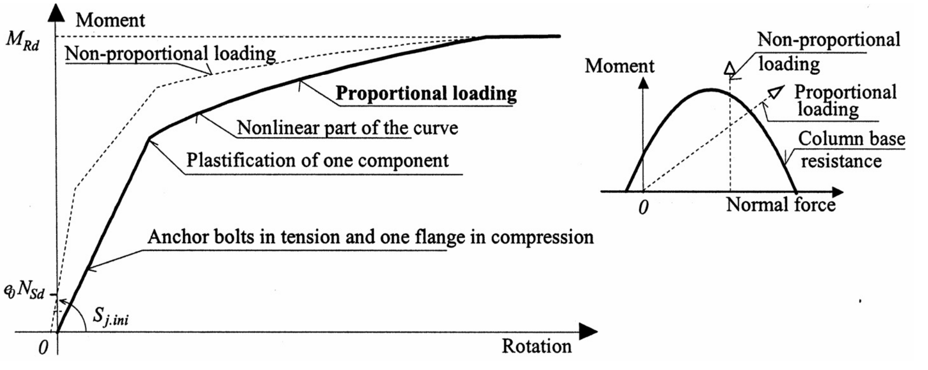

Figure 6: The moment rotation curve for the proportional loading, the non-proportional and proportional procedure on the moment -axial force diagram

The eccentricity e_0 , at which the rotation is zero, can be evaluated from Eq. (7) as

$$\phi = \frac{1}{E z^2} \left(\frac{M_{Sd}\, e_0 + N_{Sd}\, z_{c,r}}{k_{t,l}} + \frac{M_{Sd}\, e_0 - N_{Sd}\, z_{t,l}}{k_{c,r}} \right) = 0 , \tag{8}$$

hence the eccentricity under zero rotation is

$$e_0 = \frac{z_{c,r}\, k_{c,r} - z_{t,l}\, k_{t,l}}{k_{c,r} + k_{t,l}} . \tag{9}$$

The bending stiffness of a base plate depends on the bending moment due to the change of the eccentricity of the axial force

$$S_{j,ini} = \frac{M_{Sd}}{\phi} . \tag{10}$$

The base plate stiffness shell be derived based on above formula

$$S_{j,ini} = \frac{M_{Sd}}{M_{Sd} + N_{Sd}\, e_0} \frac{E z^2}{\sum \frac{1}{k}} = \frac{e}{e + e_0} \frac{E z^2}{\sum \frac{1}{k}} \ . \tag{11}$$

The non-linear part of the curve can be modelled using the shape factor μ, which depends on the bending moment as well as on the axial force in the connection as

$$\mu = \left(1,5 \frac{M_{Sd}}{M_{Rd}} \right)^{2,7} \geq 1 \ , \tag{12}$$

is leading to expression for the joint stiffness

$$S_j = \frac{e}{e + e_0} \frac{E z^2}{\mu \sum \frac{1}{k}} \ . \tag{13}$$

3.4 *Comparison to tests*

The simplified assembly procedure described in this paper together with the models of the strength and stiffness of the components as given in [10] has been implemented in a spreadsheet. Predictions have been prepared of the moment rotation curves of three series of tests carried out by Guisse [13], Wald [14] and Vandegans [15] under the project COST C1 to investigate the base plate stiffness. The predicted moment rotation curves have been compared with the test curves. In the prediction, the measured properties of the materials have been adopted without partial safety factors.

The results of the comparison of the model with the test series by Wald [14] and Vandegans [15] are reported in Figures 7 to 22. In case of the non-proportional loading, first the design moment M_{Rd} and the design axial force N_{Rd} has been calculated based on the methods given in this paper. Then, first applying the design axial force to the model N_{Rd} and then with different load steps the moment M_{Sd} from 0 to M_{Rd} simulates the non-proportional loading in the model. The value of N_{Rd} is in general somewhat lower then the axial force actually applied in the test, because M_{Rd} / N_{Rd} is taken equal to M_{Sd} / N_{Sd} . In general, despite all simplifications, the model shows good agreement with the test.

Only in case of a very high axial force, e.g. test S220-190 [15], see Figure 17, the model is conservative. This could be expected because the model of the prediction of the concrete crushing resistance is very conservative due to the concrete material variation. In this case is also conservatively neglected the contribution of the web to the load carrying capacity of the base plate in the assembly model. It should be noted that the model works equally well in the cases where there is one bolt row between the column flanges and in the cases where the bolt rows are outside the flanges, see tests S220 Figures 13 - 22.

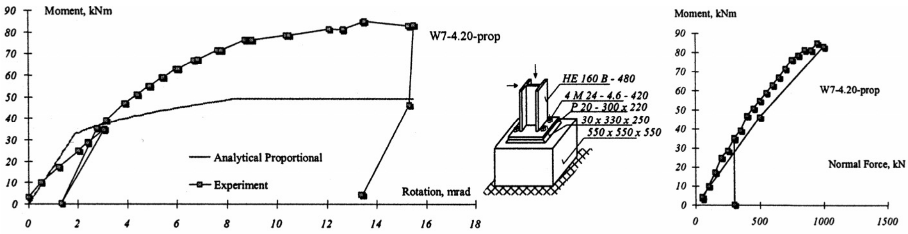

Figure 7: Experimental and predicted moment -rotational diagrams for the shown axial force history, experiment W7-4.20-prop, see [14]

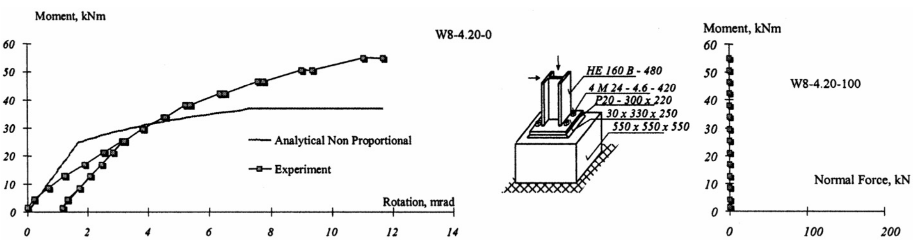

Figure 8: Experimental and predicted moment -rotational diagrams for the shown axial force history, experiment W8-4.20-const0, see [14]

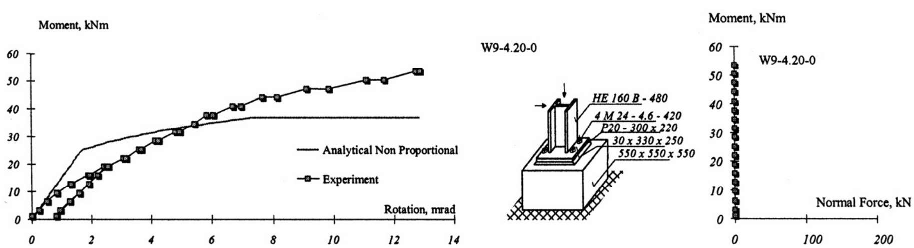

Figure 9: Experimental and predicted moment -rotational diagrams for the shown axial force history, experiment W9-4.20-0, see [14]

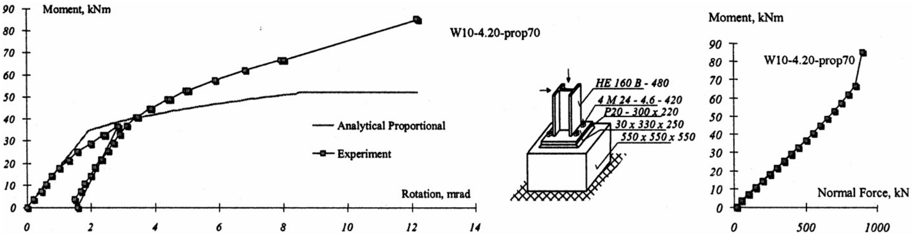

Figure 10: Experimental and predicted moment-rotational diagrams for the shown axial force history, experiment W10-4. 20-prop70, see [14]

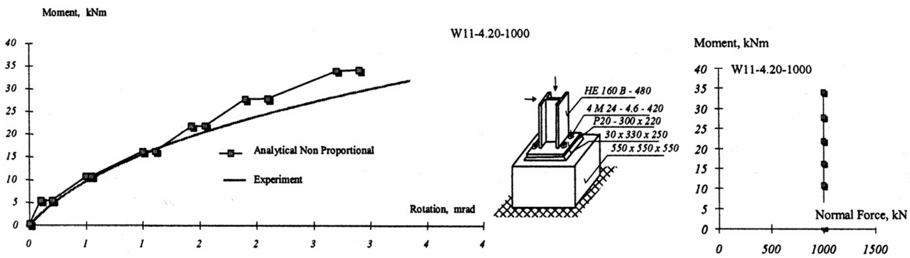

Figure 11: Experimental and predicted moment-rotational diagrams for the shown axial force history, experiment W11-4.20-1000, see [14]

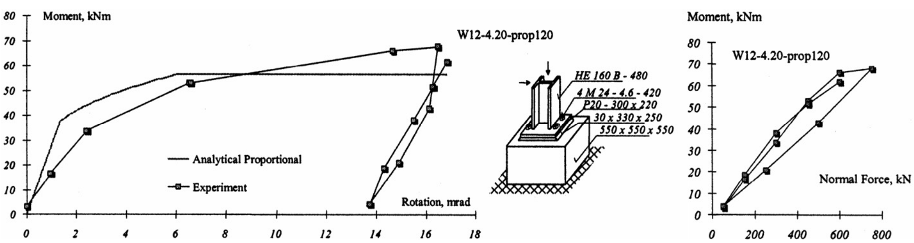

Figure 12: Experimental and predicted moment-rotational diagrams for the shown axial force history, experiment W12-4.20-prop120, see [14]

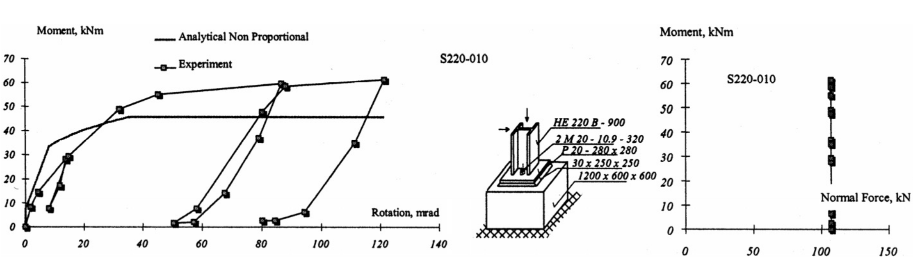

Figure 13: Experimental and predicted moment-rotational diagrams for the shown axial force history, experiment S220-010, see [15]

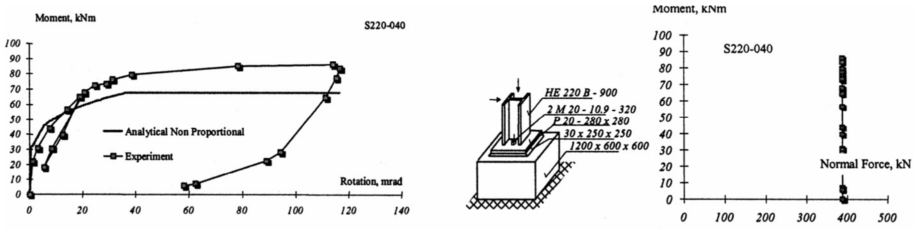

Figure 14: Experimental and predicted moment-rotational diagrams for the shown axial force history, experiment S220-040, see [15]

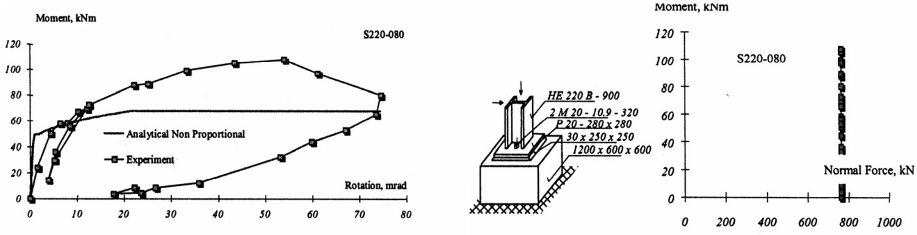

Figure 15: Experimental and predicted moment-rotational diagrams for the shown axial force history, experiment S220-080, see [15]

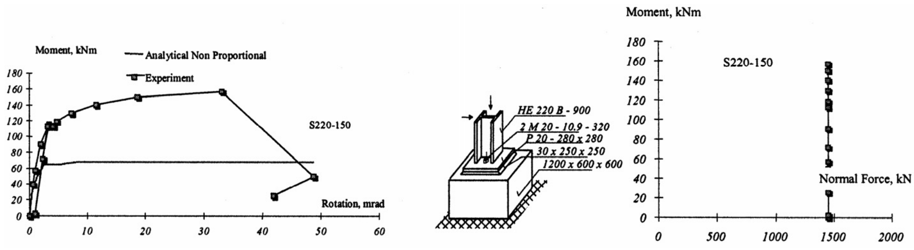

Figure 16: Experimental and predicted moment-rotational diagrams for the shown axial force history, experiment S220-150, see [15]

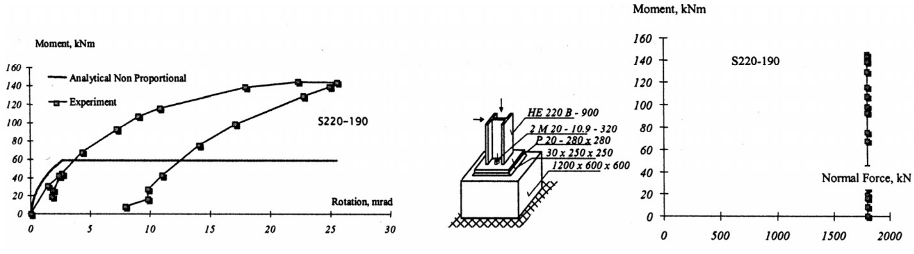

Figure 17: Experimental and predicted moment-rotational diagrams for the shown axial force history, experiment S220-190, see [15]

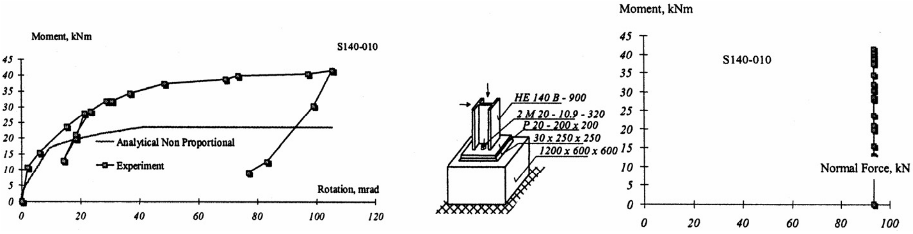

Figure 18: Experimental and predicted moment-rotational diagrams for the shown axial force history, experiment S140-010, see [15]

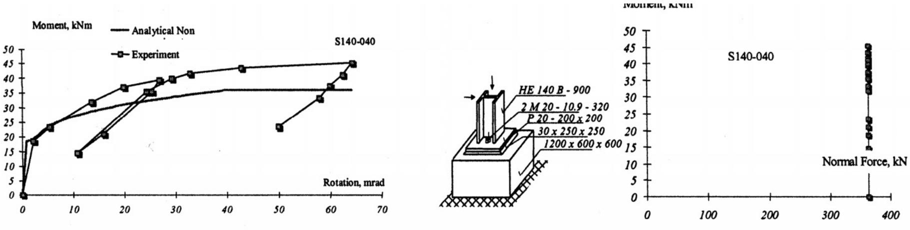

Figure 19: Experimental and predicted moment-rotational diagrams for the shown axial force history, experiment S140-040, see [15]

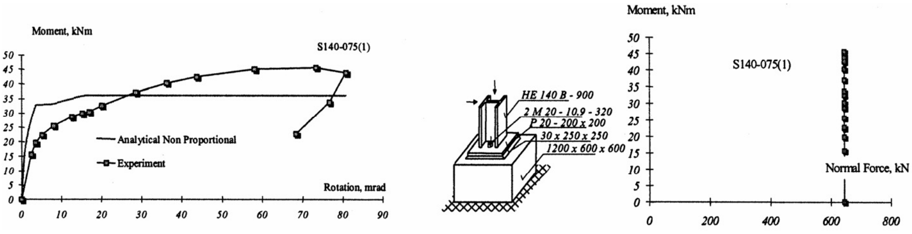

Figure 20: Experimental and predicted moment-rotational diagrams for the shown axial force history, experiment S140-075(1), see [15]

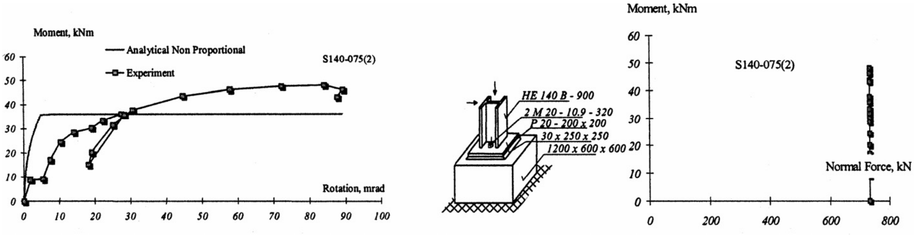

Figure 21: Experimental and predicted moment-rotational diagrams for the shown axial force history, experiment S140-075(2), see [15]

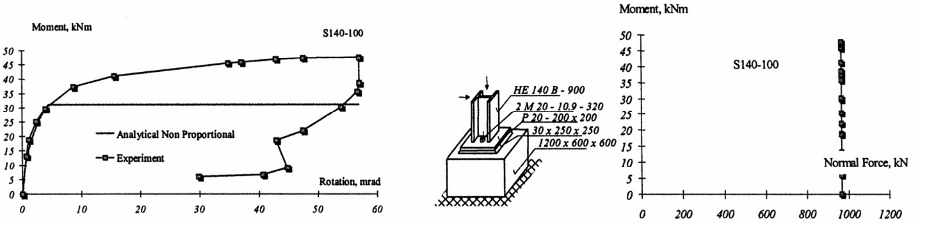

Figure 22: Experimental and predicted moment-rotational diagrams for the shown axial force history, experiment S140-100, see [15]

3.5 *Sensitivity Study*

The sensitivity of the analytical model to the base plate thickness is shown for an application, in Figure 23. It demonstrates the major influence of the tension zone resistance and stiffness on the moment rotation diagram for the non-proportional loading.

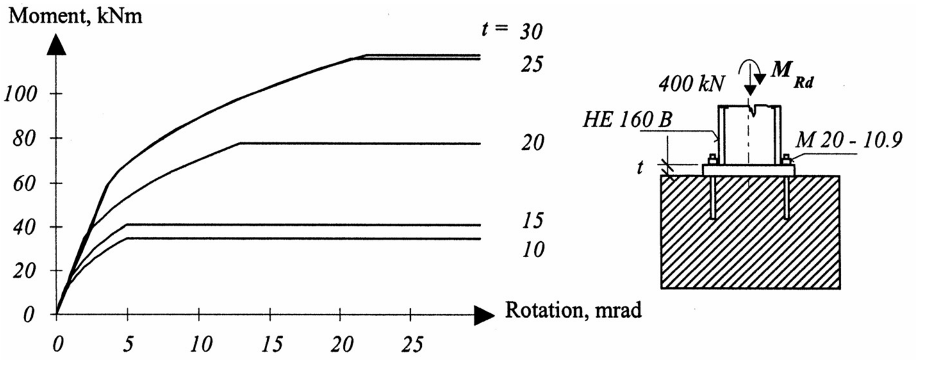

Figure 23: Moment -rotational diagram of the column base plate with the different base plate thickness for the non-proportional loading with a constant axial force

The influence of the base plate thickness is shown on Figure 24 for a column base of the column HE 200 B with a base plate 420 x 420 mm and the concrete block 1000 x 1000 mm. The column cross-section resistance in bending and compression, based on Eurocode design in Chapter 5 [3], shows the limits of the practical use of the thick base plates by the resistance of the lower part of the column loaded by the normal force and bending moment. The curve for the proportional loading is changing its inclination at the points, where the lever arm is changing from the compressed part in the concrete to the tension part in the activated bolts. The similar change of the inclination is under beginning in the case the beginning of the full tension of the column base.

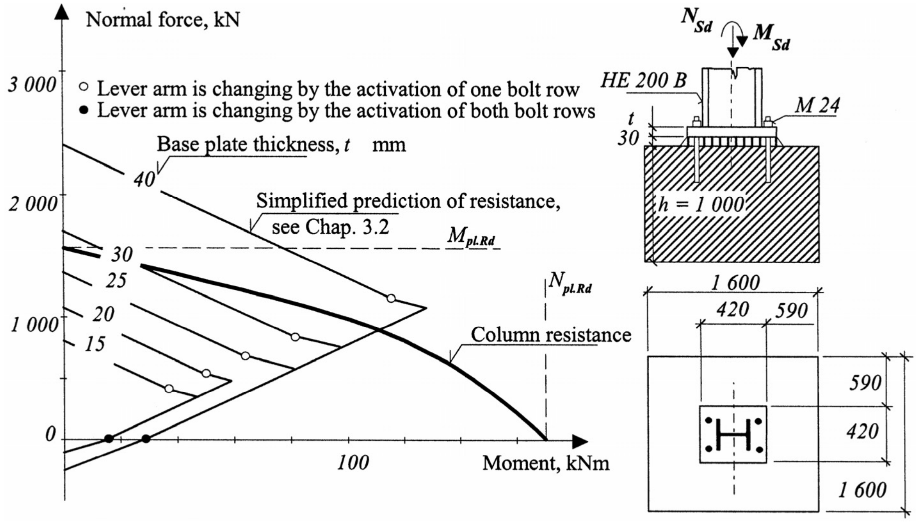

Figure 24: Comparison of the simplified (under the flanges only) model and the complex (round the column cross-section) the model of the equivalent rigid plate

The sensitivity of the column base behaviour on the anchor behaviour, which is influenced mostly by the anchor bolt elongation, is represented in Figure 25. For the test W7-4.20-prop [14] the contribution of the major components to the prediction of the bending stiffness and the resistance is also shown.

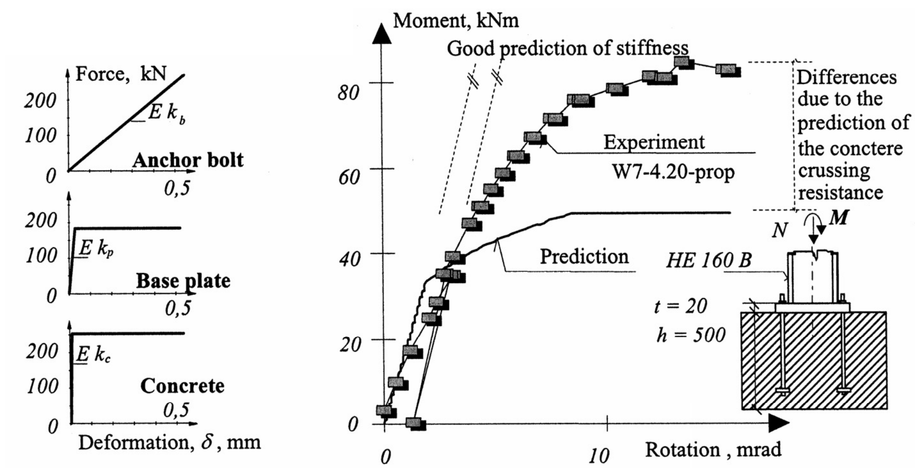

Figure 25: Comparison of the prediction model to the experiment W7-4.20-prop [14], for the load history see Figure 10, the deformation curves of each component, the moment rotational curve of the base plate connection

4 Conclusions

The model presented in this paper allows the prediction of the base plate resistance and stiffness for engineering purposes. The quality of the prediction depends on the modelling of the components.

The procedure using a proportional loading for the prediction of the bending stiffness is more suitable for the practical application compare to the prediction based on the proportional loading. Hence the prediction of the bending stiffness based on the proportional loading is recommended for practical application.

Acknowledgement

Within the framework of the European Project COST C1 (Semi-rigid behaviour of the civil engineering structural connections) and the Technical Committee 10 of ECCS (European Convention for Constructional Steelwork) an ad-hoc working group prepared a background document on design of column bases for Eurocode 3. Members of this group are: D. Brown, SCI London; A.M. Gresnigt, TU Delft; J.P. Jaspart, University of Liege; Z. Sokol, CTU in Prague; J.W.B. Stark, TU Delft; C.M. Steenhuis, TU Eindhoven; J.C. Taylor, SCI London; F. Wald, CTV in Prague (convener of the group), K. Weynand, RTWH Aachen. The work at this contribution has been supported by the grant MSM 6840770005.

References

[1] Stockwell, F. W. Jr.: Preliminary Base Plate Selection. *Engineering Journal AISC*, Vol. 21, No. 3, 1975, pp. 92-99.

[2] Bijlaard, F. S. K.: *Rekenregels voor het ontwerpen van kolomvoetplaten en experimentele verificatie.* Rapport No. BI-81-51/63.4.3410, IBBC-TNO, Delft 1982.

[3] prEN-1993-1-8, Eurocode 3, *Design of Steel Structures -General rules and roles for buildings, Part 1.8 -Joint design*. Stage 49, CEN, Brussels 2003, p. 130.

[4] DeWolf J. T, Sarisley E. F.: Column Base Plates with Axial Loads and Moments. *Journal of the Structural Division ASCE*, Vol. 106, No. ST11, 1980, pp. 2167-2185.

[5] Hogan T. J., Thomas I. R.: *Design of Structural Connections.* Australian Institute of Steel Construction, A.C.N. 000973 839, Sydney 1990.

[6] Lescouarc', H Y.: Les pieds de poteaux encastres en acier. CTICM, Avril. St. Rémy-lés-Chevreuse 1988, p. 220.

[7] Sokol Z., Wald F.: *Experiments with T-stubs in Tension and Compression*. Research Report, ČVUT, Prague 1997.

[8] Treiberg, T.: *Pelarfot*. in Swedish, Base plates, Staalbyggnadsinstitutet, Pub. 101, Stockholm 1987, p. 99.

[9] Ermopoulos J. Ch., Stamatopoulos G.N., Owens G.W.: *Influence of support conditions on the behaviour of steel frames*. in Steel Structures -Eurosteel 95, Kounadis ed., Balkema, Rotterdam 1995, pp. 211-217.

[10] *Column Bases in Steel Building Frames*. COST C1, ed. K. Weynand, Brussels, 1999.

[11] Wald F.: *Patky Sloupů -Column Bases*. ČVUT, Prague 1995, p. 137, ISBN 80-01-01337-5.

[12] Steenhuis, C.M.: *Assembly Procedure for Base Plates*. TNO Building and Construction Research Report 98-R-0477, Delft 1998.

[13] Guisse S., Vandegans D., Jaspart J.P.: *Application of the Component Method to Column Bases -Experimentation and Development of a Mechanical Model for Characterisation*. Research Centre of the Belgian Metalworking Industry, MT 195, Brussels 1996, p. 91.

[14] Wald F., Sokol Z., Šimek I., Bazantová Z.: *Column Base Semi-Rigid Behaviour*. Poddajnost patek ocelorych skeletů, in Czech, Report G 8118, CTU, Praha 1995.

[15] Vandegans D.: *Column Bases: Experimentation and Application of Analytical Models*. Research Centre of the Belgian Metalworking Industry, MT 196, p. 80, Brussels 1997.

[16] Wald F., Baniotopoulos Ch. C.: *Numerical modelling of column base connection*, in COST C1 Conference Liege 1998, s. 497-507, Brussels 1999, ISBN 92-828-6337-9.

[17] Nakashima, S.: Steel Column Bases in Japan: Experimental Research and Design Practice. In *Proceedings of the Second State of the Art Workshop COST C1*, ed. Wald F., Brussels 1994, pp. 247-258.

Symbols

e	eccentricity
k	component stiffness coefficient
z	lever arm
E	Young's modulus of steel
F	force
M	bending moment
N	axial force
S	stiffness
δ	component deformation
ϕ	connection rotation
μ	shape factor
ν	eccentricity factor

Subscripts

c	compression
j	joint
l	left
r	right
t	tension
Rd	design resistance
Sd	acting
0	under zero rotation